JOURNAL OF MATERIALS SCIENCE 31 (1996) 2515–2521

A new approach to the effective viscosity of suspensions

Z. FAN
Oxford Centre for Advanced Materials and Composites, Department of Materials, The University of Oxford, Parks Road, Oxford, OX1 3PH, UK

A. R. BOCCACCINI
School of Metallurgy and Materials, The University of Birmingham, Edgbaston, Birmingham, B15 2TT, UK

Study of the effective viscosity of suspensions is not only of interest in science, but also of great practical relevance to industries, such as the petrochemical industry, food and nutrition, materials processing and so on. In this paper, an attempt is made to establish theoretically the correlation between the effective viscosity of suspensions and their microstructural features. Firstly, the method for microstructural characterization developed by Fan *et al.* will be introduced to describe effectively the particle distribution in a suspension, and then the analogy between viscosity and field properties will be used to develop a new approach for the effective viscosity of suspensions. The new approach considers implicitly the effects of size, shape, orientation and distribution of the solid particles within the suspension through the topological parameters. Therefore, it can be applied to a suspension containing solid particles with any size, shape, orientation and distribution. Compared with other models available in the literature, the present approach is more realistic and more versatile. It can be applied to both liquids containing solid particles with a very high viscosity, and porous suspensions where the second phase has a vanishing viscosity. Perhaps more importantly, the present approach can predict the well-known S-shaped logη–volume fraction curve in the whole range of microstructures (from completely continuous to completely discontinuous) and is in better agreement with experimental results.

1. Introduction

Suspension normally refers to mixtures of at least one liquid and one dispersed solid phase. However, a liquid containing a dispersed gaseous phase can also be treated as a suspension (porous suspension) as far as the effective viscosity of the phase mixtures is concerned. Study of viscosity of suspensions is not only a matter of science, but also of great practical concern in industries, such as the petrochemical industry, food and nutrition, composite materials processing, sintering of powder compacts and so on. However, the theory of viscosity of suspensions is not well developed [1, 2]. Until now, the theoretical treatments of viscosity of suspensions have been mainly concentrated in relatively dilute suspensions containing spherical solid particles [1], and they can be classified into two categories: hydrodynamic approaches and analogous approaches. The hydrodynamic approaches are based on hydrodynamic principles, and have been reviewed in detail by Saltzer and Schulz [2]. Those approaches either try to extend Einstein's exact relationship [3] for dilute spherical suspensions to high concentrations of the solid phase [4, 5], or intend to treat the effect of non-spherical particles [6–8], or aim to consider the interaction between individual particles on the hydrodynamic behaviour of a suspension [9–11]. On the other hand, the analogous approaches utilize the mathematical analogy between field properties and viscous flow of suspensions, and treat the effective viscosity as a field property. Therefore, the equations derived for field properties can be directly applied to calculate the effective viscosity of suspensions [1, 2]. It has already been concluded by Saltzer and Schulz [2] that up to now, there is no theoretical treatment which is capable of calculating the relative viscosity of suspensions with non-spherical particles at high volume fraction of the solid phase. It is now generally believed that a realistic theoretical treatment of the effective viscosity of suspensions has to address the influence of size, shape, orientation and distribution of the solid particles in the liquid phase on the behaviour of viscous flow [1, 2].

In this paper, the analogous approach will be used to derive a new equation for predicting the effective viscosity of suspensions. In contrast to the previous models, the new approach considers implicitly the effects of size, shape, orientation and distribution of the solid particles within the suspension. Therefore, it

0022–2461

can be applied to a suspension containing solid particles with any size, shape, orientation and distribution. In addition, the new equation can also be directly applied to porous suspensions. Finally, a comparison will be made between theoretical predictions and experimental results from the literature.

2. Microstructural characterization

The quantitative characterization of a two-phase microstructure involves analysis of both geometrical and topological quantities. The geometrical characterization is well established and has been reviewed extensively by Underwood [12]. This usually involves the analysis and measurement of grain size, volume fraction and particle spacing. However, the topological characterization of a two-phase microstructure is inherently more difficult. In a previous attempt, Fan *et al.* [13] developed a series of topological parameters, such as separation, separated volume, degree of continuity and degree of separation, based on the topological parameters, contiguity and continuous volume proposed by Gurland and co-worker [14, 15]. These topological parameters can be either measured experimentally or calculated theoretically under certain simplified assumptions about the real microstructure [13]. The combination of such topological parameters can offer an effective description of the phase distribution in any two-phase microstructure.

According to the proposed topological transformation [13], a two-phase microstructure (denoted as α–β hereafter) with any grain size, grain shape and phase distribution, as illustrated schematically in Fig. 1a, can be transformed topologically into a body with three microstructural elements aligned in parallel, which is illustrated schematically in Fig. 1b. Element I (EI) consists of the continuous α-phase with a volume fraction of $f_{\alpha c}$ (the continuous volume of the α-phase); element II (EII) consists of the continuous β-phase with a volume fraction of $f_{\beta c}$ (the continuous volume of the β-phase); element III (EIII) consists of the long-range α–β chains. Therefore, there are only phase boundaries in EIII. The volume fraction of EIII is defined by the degree of separation, F_S. The volume

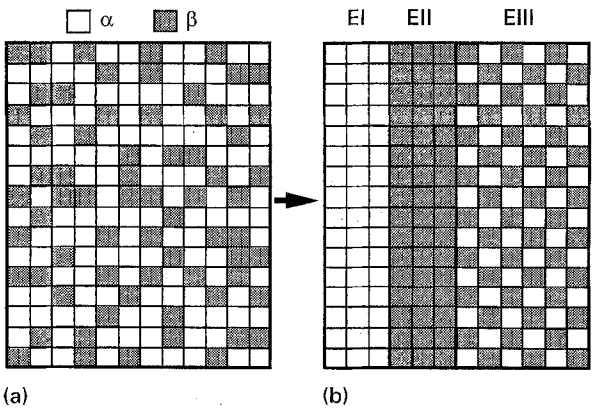

Figure 1 Schematic illustration of the topological transformation from (a) microstructure A to (b) microstructure B [13]. It should be emphasized that this graph is just a "schematic" illustration of the topological transformation and does not represent any quantitative information such as volume fraction, grain size and grain shape.

fractions of the α-phase ($f_{\alpha III}$) and β-phase ($f_{\beta III}$) in EIII body can be calculated by the following equations

$$f_{\alpha III} = \frac{f_\alpha - f_{\alpha c}}{F_s} \quad (1)$$

$$f_{\beta III} = 1 - f_{\alpha III} \quad (2)$$

As was discussed in detail elsewhere [13, 16–20], microstructures A and B (see Fig. 1) are mechanically equivalent along the aligned direction of microstructure B. As far as the field properties are concerned, taking electrical conductivity as an example, microstructures A and B are also equivalent along the aligned direction provided that the electrical current I of the applied electrical field is along this same direction [21]. As a consequence of this topological transformation, the determination of the effective field properties of a complicated two-phase microstructure can be replaced by an analysis of the simpler but equivalent microstructure with three well-defined microstructural elements.

The following aspects on microstructural characterization need further explanation:

1. The topological parameters developed by Fan *et al.* [13] were derived by means of statistics and probability theory, and hence they have to be treated in terms of averages and statistics. They reflect implicitly the change in size, shape, orientation and distribution of the second phase.

2. In general cases, the topological parameters have to be measured experimentally by applying a standard metallographic method described by Underwood [12]. However, under the assumption of equiaxed grain and random distribution, they can also be calculated, for example,

$$f_{\alpha c} = \frac{f_\alpha^2 d_\beta}{f_\beta d_\alpha + f_\alpha d_\beta} = \frac{f_\alpha^2 R}{f_\beta + f_\alpha R} \quad (3)$$

$$f_{\beta c} = \frac{f_\beta^2 d_\alpha}{f_\beta d_\alpha + f_\alpha d_\beta} = \frac{f_\beta^2}{f_\beta + f_\alpha R} \quad (4)$$

$$F_S = 1 - f_{\alpha c} - f_{\beta c} \quad (5)$$

where R is the grain size ratio and is defined as $R = d_\beta/d_\alpha$.

3. In cases where experimentally measured topological parameters are not available, the following power law can be used to approximate the continuous volumes:

$$f_{\alpha c} = f_\alpha^m \quad (6)$$

$$f_{\beta c} = f_\beta^n \quad (7)$$

For example, the experimentally measured continuous volume of the WC phase in Co–WC composites [15, 22] can be adequately represented by $n = 4$ [16].

4. Topological parameters are directional [13]. The measurement of all the topological parameters of a given composite with specific microstructural features must be made along the direction of the field intensity (e.g. the electrical current I). In addition, the topological transformation must also be made along this same direction.

3. The effective viscosity of suspensions

A group of physical properties, such as moduli of elasticity, electrical conductivity, dielectric constant, magnetic permeability, thermal conductivity, diffusion coefficient and so on, are governed by the same form of constitutive equations, and are therefore mathematically analogous [23]. This group of physical properties of composite materials are usually referred to as the effective field properties or transport properties in the literature [24]. Consequently, a theoretical solution to any field property within the group can be applied to other field properties by direct analogy [23–25].

Field property in general can be defined by equations of the following type

$$\dot{\mathbf{q}} = -\Phi \nabla T \tag{8}$$

where $\dot{\mathbf{q}}$ is a flow density, $T = T(x, y, z)$ a three-dimensional field, and Φ an effective field property. Meanwhile, the viscosity of Newtonian flow, η, is defined by the following equation

$$\tau_{xz} = \eta \frac{dv}{dy} \tag{9}$$

where τ_{xz} is the shear stress in the (x, z) plane, and dv/dy the velocity gradient in y direction. Thus, one can modify Equation 9 for steady laminar flow of an incompressible fluid in such a manner that the direct analogy between Equations 8 and 9 is obvious [2]. In fact, such analogy was found as early as 1900 by Cohn [26] and later by Lamb [27] and Maruhn [28]. They found that the laws governing the potential flow are identical to those for the electrostatic field. Therefore, the viscosity of suspensions can be treated as a field property.

In previous work, Fan [21, 29] has derived the following equation to describe the effective field property (Φ^c) of a two-phase composite (α–β) as functions of the field properties of the constituent phases (Φ^α and Φ^β) and topological parameters of the composite:

$$\Phi^c = \Phi_\alpha f_{\alpha c} + \Phi_\beta f_{\beta c} + \frac{\Phi_\alpha \Phi_\beta F_s}{\Phi_\beta f_{\alpha III} + \Phi_\alpha f_{\beta III}} \tag{10}$$

where the subscripts α and β denote α and β phases. Equation 10 is applicable to a two-phase composite with any combination of volume fraction, particle size, shape and distribution. It has been shown that the predictions for various field properties by Equation 10 are in good agreement with experimental data [21, 29]. By the direct analogy discussed previously, the effective viscosity (η^c) of a suspension (liquid α containing solid β particles) can therefore, be, described in terms of viscosity of the constituent phases (η_α and η_β) and the topological parameters by the following equation:

$$\eta^c = \eta_\alpha f_{\alpha c} + \eta_\beta f_{\beta c} + \frac{\eta_\alpha \eta_\beta F_s}{\eta_\beta f_{\alpha III} + \eta_\alpha f_{\beta III}} \tag{11}$$

Similarly, Equation 11 can also be applied to a suspension with any combination of volume fraction, size, shape and distribution of the solid particles.

Normally, in a suspension, the viscosity of the dispersed phase (solid particles) is much higher than that of the liquid matrix, i.e. $\eta_\beta \gg \eta_\alpha$. However, as a special case of suspension, the gaseous phase in a powder compact during sintering has a much lower viscosity than the matrix, being very close to zero ($\eta_\beta \approx 0$). Thus, one obtains the following equation for the viscosity of a porous suspension, η^p:

$$\eta^p = \eta_\alpha f_{\alpha c} \tag{12}$$

or

$$\eta_r = \frac{\eta^p}{\eta_\alpha} = f_{\alpha c} \tag{13}$$

where η_r is the normalized viscosity of porous suspensions. It is very interesting to note in Equation 13 that the normalized viscosity of a porous suspension is simply equal to the continuous volume of the liquid phase.

4. Comparison with experimental results

4.1. Suspensions with solid dispersions

The measurements of the viscosity of glass melts containing solid dispersion were carried out recently by one of the authors [30] in a Searle-type rotation viscometer, which was calibrated using the standard glass I (soda-lime glass) of the German Glass Society (DGG) in the temperature range of 1273–1773 K. The two suspensions of interest here are Na_2O–SiO_2 melts containing SiO_2 particles at 1773 K and Na_2O–GeO_2 melts containing GeO_2 particles at 1273 K. At 1773 K SiO_2 particles have a hexagonal crystal structure (trydimite) with a nearly equiaxed morphology (aspect ratio is about 1.25) [31], while GeO_2 particles at 1273 K are rutile with a more elongated morphology (aspect ratio is about 3) [32, 33]. The measured viscosity data are presented as a function of the volume fraction of the solid phase in Fig. 2 for Na_2O–SiO_2 melts

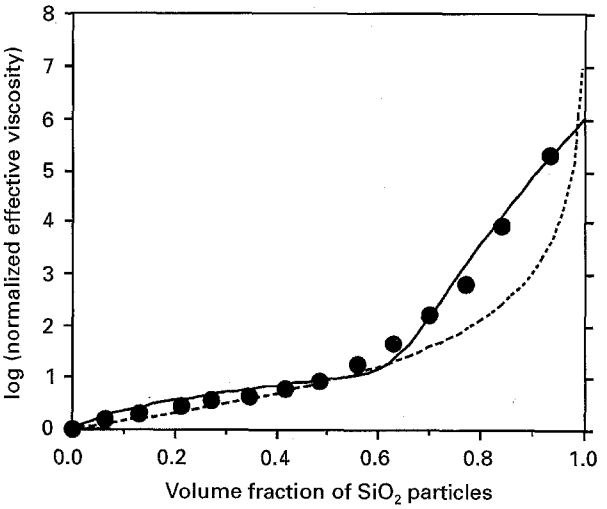

Figure 2 The theoretically predicted normalized effective viscosity of Na_2O–SiO_2 melt containing SiO_2 solid particles at 1773 K by the present approach in comparison with the experimental data from Boccaccini *et al.* [30]. Also shown here are the theoretical predictions by Saltzer and Schulz's model [1]. Key: ● Experimental Boccaccini *et al.* [30]; ----- Saltze and Schulz's model [1]; —— this approach.

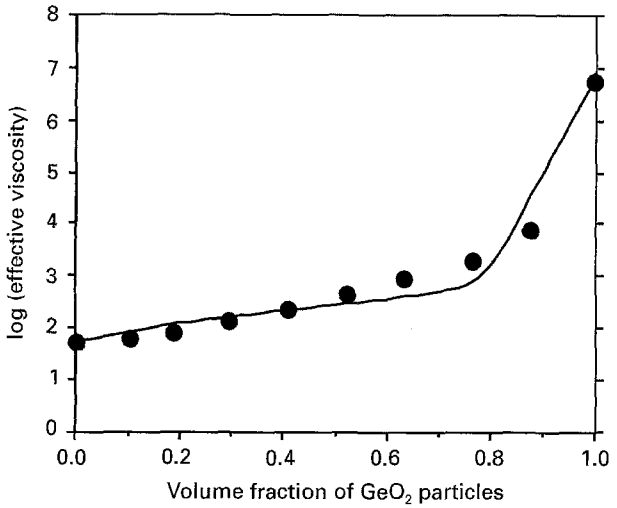

Figure 3 The theoretically predicted effective viscosity of Na_2O–GeO_2 containing GeO_2 solid particles at 1273 K by the present approach in comparison with the experimental data from Boccaccini *et al.* [30]. Key: ● Exp. Boccaccini *et al.* [30]; —— this calculation.

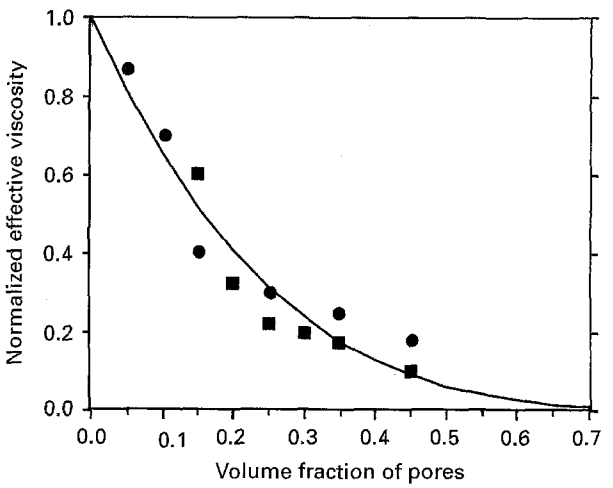

Figure 4 The theoretically predicted normalized effective viscosity of porous glasses as a fuinction of volume fraction of pores by the present approach in comparison with the experimental data from literature. ● for commercial aluminosilicate [35], ■ for cordierite-type glass [36] and —— this calculation.

containing SiO_2 particles at 1773 K and in Fig. 3 for Na_2O–GeO_2 melts containing GeO_2 particles at1273 K.

To apply the present approach to the above two suspensions, we need to know the topological parameters ($f_{\alpha c}$, $f_{\beta c}$ and F_s) which characterize the distribution of the solid particles in the melt. Unfortunately, experimentally measured topological data are not available for these two systems in the literature. However, as already mentioned in Section 2, they can be estimated by assigning the m and n values in Equations 6 and 7. Compared with a solid two-phase structure having a random distribution where m and n have a value around 4, the solid particles in a suspension at high temperature are much more separated than the liquid phase. Thus, we choose $m = 1.1$ and $n = 25$ for Na_2O–SiO_2 melts containing SiO_2 particles at 1773 K, and $m = 1.1$ and $n = 40$ for Na_2O–GeO_2 melts containing GeO_2 particles at 1273 K. The viscosity data for each constituent phase are from the experimental results by Boccaccini *et al.* [30]. The theoretical predictions of Equation 11 are compared with the experimental data in Figs 2 and 3 for Na_2O–SiO_2 and Na_2O–GeO_2 suspensions, respectively. Figs 2 and 3 indicate that the theoretical predictions are in good agreement with the experimental data in the whole range of volume fraction of the solid particles. It is very interesting to note that the theoretical predictions with the present approach in Fig. 2 follow the exact variation trend of the experimental data.

4.2. Porous glasses

In glass suspensions the viscosity of the solid dispersoids are much higher than that of the liquid phase. In contrast, in the porous glass (a porous suspension) the dispersoids (gas) at the sintering temperature have a vanishing viscosity. It is of great interest to be able to understand the effect of gaseous dispersoids on the viscous flow of porous glass during sintering, i.e. the densification, forming and creep behaviour at high temperature [34–37].

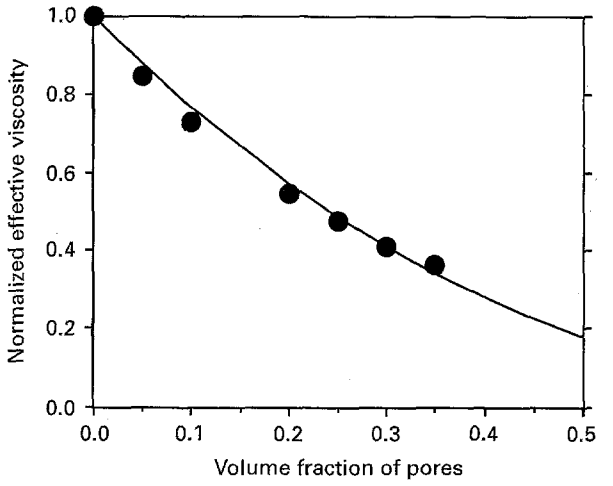

Figure 5 The theoretically predicted normalized effective viscosity of a porous suspension (soda-lime glass) as a function of volume fraction of pores by the present approach in comparison with the experimental data [37]. Key: ● experimental Rahaman and De Jonghe [37]; ——— this calculation.

However it is difficult to characterize experimentally the pore size, shape and distribution in porous glass at the sintering temperature [30]. Therefore, we will choose the m value in Equation 6 to approximate the pore distribution. For cordierite-type glass and commercial Corning glass the value 3.5 is assigned to m in Equation 6, and for soda-lime glass $m = 2.5$. The theoretically predicted normalized viscosities of different porous glasses from Equation 13 are presented in Figs 4 and 5 in comparison with corresponding experimental data [35–37]. It is shown in Figs 4 and 5 that the theoretical predictions are in fairly good agreement with the experimental data.

5. Discussion

5.1. Comparison with other theoretical models

There are a number of theoretical models available in the literature for the effective viscosity of suspensions.

However, most of them are either empirical or developed only for specific suspensions at low volume fraction of solid particles [2]. Perhaps the most useful model is the one proposed by Saltzer and Schulz [1]. Therefore, in this section, their model will be introduced briefly and will be compared with the present approach.

By analogy to the field properties of two-phase materials developed by Niesel [38], Saltzer and Schulz [1] proposed the following equation for the relative effective viscosity ($\eta_r = \eta_c/\eta_{liquid}$) of suspensions at the limit of $\eta_{liquid}/\eta_{solid} \to 0$

$$\eta_r = (1-f)^{-q}, \quad q = \frac{1-\cos^2\alpha}{F} + \frac{\cos^2\alpha}{1-2F} \tag{14}$$

where f is the volume fraction of the solid phase, $F(0 < F < 0.5)$ is a shape factor which is a function of the aspect ratio of the solid particles, and $\cos^2\alpha$ $(0 < \cos^2\alpha < 1)$ is the orientation factor. For Na_2O–SiO_2 melts containing SiO_2 particles at 1773 K, it was shown that $F = 0.3$, $\cos^2\alpha = 1/3$ [30]. The theoretical predictions for Na_2O–SiO_2 melts containing SiO_2 particles at 1773 K by both the present approach (Equation 11 and Equation 14) are shown in Fig. 2 in comparison with the experimental results [30]. Fig. 2 indicates that the present approach can achieve good agreement with experimental data over the whole range of volume fraction of the solid phase, while Equation 14 can only offer predictions with a reasonable accuracy for dilute suspensions ($f < 0.6$). The main reason for the discrepancy lies in the difference in microstructural considerations by the two approaches. Saltzer and Schulz's approach [1] (Equation 14) considers explicitly the effects on viscosity of the shape and orientation of solid particles, but it does not consider the effect of solid particle distribution in the liquid phase, while the present approach (Equation 11) considers not only the effect of solid particle distribution, but also the effects of shape and orientation of solid particles implicitly through three topological parameters ($f_{\alpha c}$, $f_{\beta c}$ and F_s) [13]. It can be demonstrated that the effect of solid particle distribution in the liquid phase on the flow behaviour of suspensions can be crucial (see Section 5.2).

In addition, the present approach treats the viscosity of the dispersed phase at the temperature of concern as a factor for consideration, which reflects the physical nature of the dispersed phases, and consequently, Equation 11 can be applied to any suspension irrespective of the viscosity of the constituent phases. In contrast, Saltzer and Schulz's approach can only be applied to suspensions where $\eta_{liquid}/\eta_{solid} \to 0$.

To sum up, in comparison with Saltzer and Schulz's model, the basic considerations by the present approaches more closely the real situation for the flow behaviour of suspensions, and therefore it can be applied to any suspension irrespective of the viscosity, size, shape, orientation and distribution of the constituent phases. The predictions by the present approach should have high accuracy once the topological parameters ($f_{\alpha c}$, $f_{\beta c}$ and F_s) are properly measured by experiment.

5.2. The effect of the solid particle distribution on the viscosity of suspensions

A large number of experimental data for the viscosity of suspensions are available in the literature, and are plotted in Fig. 6 as a function of the volume fraction of the solid phase. It is obvious from Fig. 6 that the experimental data have a considerable scatter, particularly at high volume fraction of the solid particles. It is now well accepted that this scatter is caused by the difference in particle distribution within different liquid suspensions [1]. In dilute suspensions, the solid particles are completely separated by the liquid phase, and the distribution of solid particles can be uniquely described as uniform ($f_{\beta c} = 0$). This explains why the scatter in experimental data at low volume fraction is not so severe. With increasing volume fraction of the solid phase, the number of solid particle contacts increases. This will result in an increase in viscosity. However, due to the difference in physical nature, size, shape, orientation and distribution of solid particles in different suspensions, the increase in viscosity will largely depend on the characteristics of specific suspensions, which gives rise to the considerable scatter at high volume fraction in Fig. 6. Therefore, any realistic theoretical approach to the viscosity of suspensions has to consider the effect of particle arrangement. The present approach (Equation 11) has a provision for the evaluation of such a microstructural effect.

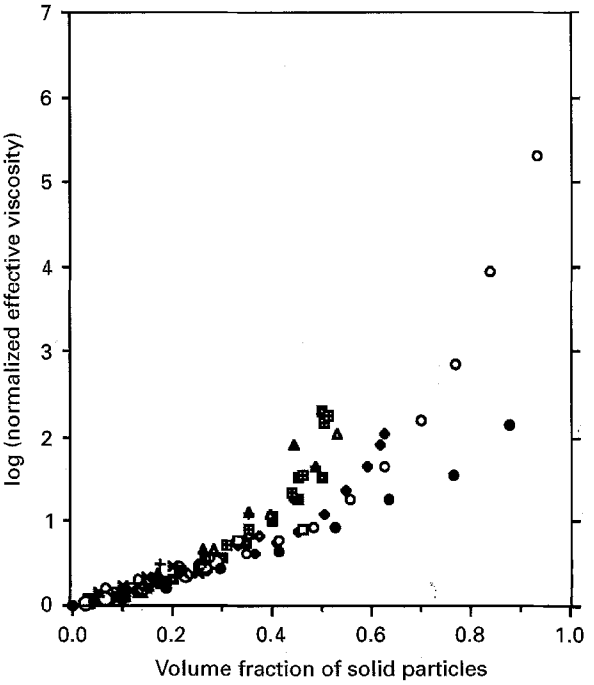

Figure 6 Experimentally measured normalized effective viscosity of suspensions as a function of volume fraction of solid particles. Key: ⊡ Eirirch *et al.* [39,40]; ◆ Eilers [41]; ■ Vand [10]; ◇ Robinson [42]; □ Robinson [44]; ▲ Williams [45]; ▲ Sweeny and Geckler [46]; ○ Higginbotham *et al.* [47]; + Nicodemo *et al.* [48]; ▦ Van Kao *et al.* [49]; × Schulz [50]; ✖ Saltzer and Schulz [1]; ○ Boccaccini *et al.* [30]; ▣ Ward and Whitmore [43]; ● Boccaccini *et al.* [30].

If we assume that there is a liquid suspension, where $\eta_{solid}/\eta_{liquid} = 10^9$, and the continuous volume of the liquid phase can be approximated by $m = 1.1$ in Equation 6, the effect of solid particle distribution on the effective viscosity of the suspension can be evaluated by changing the n parameter in Equation 7. The calculated results are presented in Fig. 7 as a function of volume fraction of the solid phase and the n parameters, which are indicated by the data attached to each line. There are two extreme cases: one is $n = 1$ ($f_{\beta c} = f_\beta$) which physically means that all the solid particles are completely continuous; the other one is $n = \infty$ ($f_{\beta c} = 0$) which represents a suspension where all the solid particles are completely discontinuous. When $1 < n < \infty$, the solid phase is partially continuous, and the larger the n value is the more discontinuous the solid phase is. For a given n value (e.g. $n = 20$), Equation 11 actually predicts the well-known S-shaped logη–volume fraction curve. The effective viscosity of dilute suspensions increases slowly with increasing volume fraction of the solid particles until it reaches a critical volume fraction where viscosity increases sharply with further increase of volume fraction, while at high volume fraction, this increase in viscosity will slow down again. At a given volume fraction, the effective viscosity of a suspension increases with increasing contiguity of the solid particles.

In addition, there is a very interesting point in Fig. 7 worth noting. At low volume fraction of the solid phase, irrespective of the n value used, the predicted effective viscosity always coincides with the line predicted by $n = \infty$. The two lines separate at a critical volume fraction, f^*. Since $n = \infty$ defines a suspension in which the solid particles are completely discontinuous (no particle contact), for a given n value, f^* defines the volume fraction at which solid particles start to make contact with each other. Once the volume fraction exceeds f^*, the effective viscosity increases sharply with further increase of volume fraction. The calculated f^* values at $m = 1.1$ are plotted in Fig. 8 as a function of the n parameter. There are two limiting cases: one is $f^* = 0$ corresponding to $n = 1$; the other is $f^* = 1$ corresponding to $n = \infty$. In general cases ($1 < n < \infty$), f^* increases with increasing n value (Fig. 8).

However, to evaluate quantitatively the effect of particle distribution on the effective viscosity of suspensions by experiments might be difficult. It is obvious that further experimental work is required to characterize the solid particle distribution in suspensions.

Finally, it is necessary to discuss a little further the n and m parameters in Equations 6 and 7. Although $m = n = 1$ and $m = n = \infty$ correspond to completely continuous and discontinuous microstructures as discussed previously, m and n are not microstructural parameters and have no clear physical meaning. The reason for proposing Equations 6 and 7 are three-fold. Firstly, the experimentally measured $f_{\alpha c}$ and $f_{\beta c}$ data can be adequately fitted by such a power law as demonstrated by a number of studies in two-phase alloys [51, 52]. Secondly, Equations 6 and 7 can offer us a convenient way to vary systematically the continuous volumes of the constituent phases in a two-phase structure over the whole range of volume fraction, so that the effect of particle distribution can be evaluated theoretically, as shown in Fig. 7. Finally, in systems where experimentally measured topological parameters are not available, Equations 6 and 7 can be used as a reasonable approximation of the continuous volume by choosing the right m and n values. Nevertheless, m and n are not fitting parameters in this approach, $f_{\alpha c}$ and $f_{\beta c}$, as microstructural parameters, should be measured experimentally in general.

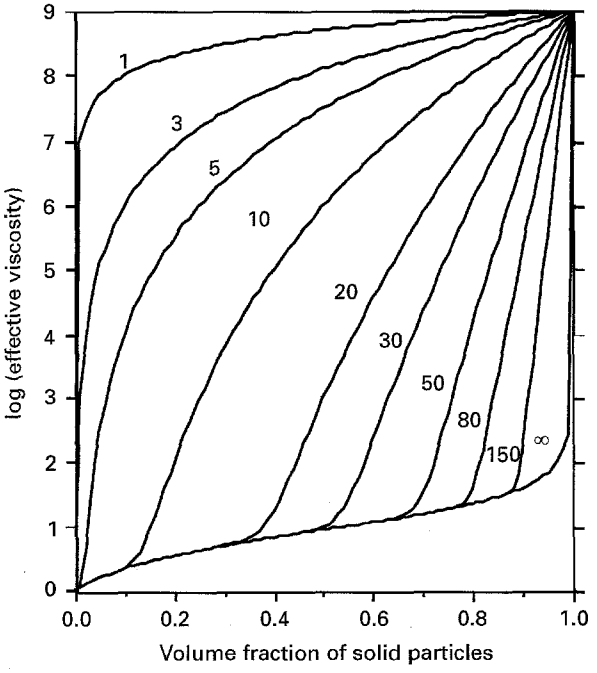

Figure 7 The theoretically calculated normalized effective viscosity of a hypothetical suspension with $\eta_{solid}/\eta_{liquid} = 10^9$ as a function of volume fraction of solid particles and the n parameter in Equation 7, which are indicated by the data attached to each line. It is also assumed that $m = 1.1$ in Equation 6.

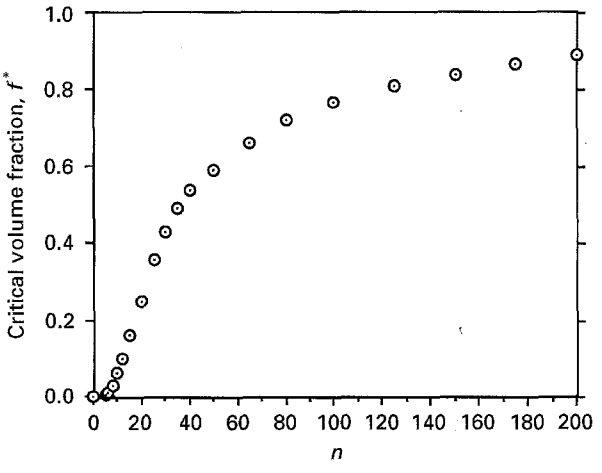

Figure 8 The theoretically calculated critical volume fraction f^* of a hypothetical suspension with $\eta_{solid}/\eta_{liquid} = 10^9$ as a function of the n parameters in Equation 7 and assuming $m = 1.1$ in Equation 6.

6. Summary

Based on the microstructural characterization method and the analogy between viscosity and field properties (or transport properties), a new approach to the effective viscosity of suspensions has been developed. The new approach can consider implicitly the effects of size, shape, orientation and distribution of the solid particles within the suspension. Therefore, it can be applied to a suspension containing solid particles with any size, shape, orientation and distribution. Compared with other models available in the literature, the present approach is more realistic and more versatile. It can be applied to both liquids containing solid particles with a very high viscosity, and porous suspensions where the second phase is a gas with a vanishing viscosity. Perhaps more importantly, the present approach can predict the well-known S-shaped logη–volume fraction curve in the whole range of microstructures (from completely continuous to completely discontinuous) and is in better agreement with experimental results. Finally, the effect of solid particle distribution on the effective viscosity of suspensions has also been demonstrated quantitatively.

Acknowledgement

The collaboration on this work between the authors was initiated by the late Professor G. Ondracek, the Director of Institut für Gesteinshuttenkunde, RWTH Aachen, Germany. We dedicate this paper to the memory of Professor Ondracek with our respect.

References

1. W. D. SALTZER and B. SCHULZ, *High Temp. High Pressure* **15** (1983) 289.
2. *Idem.* in Continuum Models of Discrete Systems: Proceedings of the 4th Conference 1981, Stockholm (North-Holland, Amsterdam), 423.
3. A. EINSTEIN, *Ann. Phys.* **19** (1906) 289.
4. H. C. BRINKMAN, *J. Chem. Phys.* **20** (1952) 571.
5. R. ROSCOE, *Br. J. Appl. Phys.* **3** (1952) 267.
6. G. B. JEFFREY, *Proc. R. Soc. London Ser. A* **102** (1923) 161.
7. A. PETERLIN, *J. Phys.* **111** (1939) 232.
8. W. KUHN, H. KUHN and P. BUCHNER, *Ergeb. Exakten Naturwiss* **25** (1951) 1.
9. E. GUTH and R. SIMHA, *Koloid Z.* **74** (1936) 266.
10. V. VAND, *J. Phys. Colloid Chem.* **52** (1948) 277.
11. R. SIMHA, *J. Appl. Phys.* **23** (1952) 1020.
12. E. E. UNDERWOOD, in "Stereology and quantitative metallography", STP 504, (ASTM, Philadelphia, PA, 1972) p. 3.
13. Z. FAN, A. P. MIODOWNIK and P. TSAKIROPOULOS, *Mater. Sci. Tech.* **9** (1993) 1094.
14. J. GURLAND, *Trans. Met. Soc. AIME* **212** (1958) 452.
15. H. C. LEE and J. GURLAND, *Mater. Sci. Eng.* **33** (1978) 125.
16. Z. FAN, P. TSAKIROPOULOS and A. P. MIODOWNIK, *Mater. Sci. Technol.* **8** (1992) 922.
17. *Idem. Ibid.* **9** (1993) 863.
18. Z. FAN, P. TSAKIROPOULOS, P. A. SMITH and A. P. MIODOWNIK, *Phil. Mag.* **67A** (1993) 515.
19. Z. FAN and A. P. MIODOWNIK, *Acta Metall. Mater.* **40** (1993) 2403.
20. *Idem. ibid.*, **40** (1993) 2415.
21. Z. FAN, *Acta Metall. Mater.* **43** (1995) 43.
22. H. FISCHMEISTER and H. E. EXNER, *Arch. Eisenhuttenwes.* **37** (1966) 489.
23. J. N. SHIRE and R. L. WEBER, "Similarities in Physics" (Adam Hilger, Bristol, 1982).
24. G. ONDRACEK, *Rev. Powder Metall. Physical Ceram.* **3** (1987) 205.
25. Z. HASHIN, in "Mechanics of Composite Materials", edited by F. W. Wendt, H. Liebowitz and N. Perrone (Pergamon Press, Oxford, 1970) p. 201.
26. E. COHN, "Das Elektromagnetische Feld" (Verlag S Hirzel, Leipzig, 1900).
27. H. LAMB, "Lehrbuch der Hydrodynamik", 2nd Edn (Teubner Verlag, Leipzig, Berlin, 1931) p. 151.
28. K. MARUHN, in "2. Jahrbuch der deutschen Luftfahrtfoschung", Vol. 1 (Verlag Oldenbourg, Munchen, Berlin, 1941) p. 135.
29. Z. FAN, *Phil. Mag.* (1996) in press.
30. A. R. BOCCACCINI, K. D. KIM and G. ONDRACEK, *Mat.-wiss. u. Werkstofftech* **26** (1995) 263.
31. F. TROJER, "Die Oxydischen Kristallphasen" (Schweizerbartsche Verlagsbuchhandlung, 1963) p. 77.
32. W. VOGEL, "Glaschemic" (Springer-Verlag, Berlin, 1992) p. 211.
33. J. WILLIAMSON and F. B. GLASER, *Science* **148** (1965) 158.
34. A. R. BOCCACCINI and G. ONDRACEK, *Glastech. Ber.* **65** (1992) 73.
35. V. C. DUCAMP and R. RAJ, *J. Amer. Ceram. Soc.* **72** (1989) 798.
36. V. SURA and P. C. PANDA, *ibid.* **73** (1990) 2697.
37. M. N. RAHAMAN and L. C. DE JONGHE, *ibid.* **73** (1990) 707.
38. W. NIESEL, *Anal. Phys. 6 Folge* **10** (1952) 336.
39. F. EIRICH, H. MARGARETHA and M. BUNZL, *Kolloid. Z.* **74** (1936), 276.
40. *Idem. ibid.* **75** (1936) 20.
41. H. Eilers, *Kolloid. Z.* **96/97** (1941) 313.
42. J. V. ROBINSON, *J. Phys. Kolloid. Chem.* **53** (1949) 1042.
43. S. G. WARD and L. R. WHITMORE, *Br. J. Appl. Phys.* **1** (1950) 286.
44. J. V. ROBINSON, *J. Phys. Kolloid. Chem.* **55** (1951) 455.
45. P. S. WILIAMS, *J. Appl. Phys.* **3** (1953) 120.
46. K. SWEENY and R. D. GECKLER, *ibid.* **25** (1954) 1135.
47. G. H. HIGGINBOTHAM, D. R. OLIVER and S. G. WARD, *Br. J. Appl. Phys.* **9** (1958) 372.
48. L. NICODEMO, C. L. NICOLAIS and R. F. LANDEL, *Chem. Eng. J.* **29** (1974) 729.
49. S. VAN KAO, S. E. NIELSEN and C. T. HILL, in "Rheology of Concentrated Suspensions", HPC-74-167 (University of Washington, Seattle, 1974).
50. B. SCHULZ, in Proceedings of ANS/ASME Meeting, Saragota, USA, NUREG/CP-0014, (American Society For Mechanical Engineers, New York, 1980) p. 1967.
51. E. WERNER and H. P. STUWE, *Mater. Sci. Eng.* **68** (1984–1985) 175.
52. P. UGGOWITZER and H. P. SUWE, *Z. Metallkd* **73** (1982) 277.

Received 18 October 1995
and accepted 20 November 1995